Cleavage of an Aryl Carbon–Sulfur Bond in Hydride–Thiolate Complexes of Molybdenum and Tungsten. Crystal Structures of $[\{Mo(SC_6H_2Pr^i_3\text{-}2,4,6)(OMe)(PMePh_2)\}_2(\mu\text{-}S)_2]$ and $[\{Mo(SC_6H_2Pr^i_3\text{-}2,4,6)(OEt)(PEtPh_2)\}_2(\mu\text{-}S)_2]$ *

Timothy E. Burrow,[a] **David L. Hughes,**[b] **Alan J. Lough,**[a] **Michael J. Maguire,**[b] **Robert H. Morris**[a] **and Raymond L. Richards**[b]

[a] *Department of Chemistry and the Scarborough Campus, University of Toronto, Toronto, Ontario M5S 1A1, Canada*

[b] *Nitrogen Fixation Laboratory, University of Sussex, Brighton BN1 9RQ, UK*

The complexes $[MoH(SC_6H_2Pr^i_3\text{-}2,4,6)_3(PR^1Ph_2)]$ **1** (R^1 = Me or Et) in tetrahydrofuran (thf)–R^2OH decomposed *via* cleavage of an aryl carbon–sulfur bond to give $C_6H_3Pr^i_3$-1,3,5 and the complexes $[\{Mo(SC_6H_2Pr^i_3\text{-}2,4,6)(OR^2)(PR^1Ph_2)\}_2(\mu\text{-}S)_2]$ **2** (R^2 = Me or Et). Compounds **2a** ($R^1 = R^2$ = Me) and **2b** ($R^1 = R^2$ = Et) have been structurally characterised by X-ray diffraction and shown to be dimers with $(\mu\text{-}S)_2$ bridging ligands derived from the thiolate ligands of the precursor complexes. The arene produced in these reactions has been detected by ^2H NMR spectroscopy and by GC–mass spectrometry; $C_6H_2(^2H)Pr^i_3$-1,3,5 was observed from $[MoH(SC_6H_2Pr^i_3\text{-}2,4,6)_3(PR^1Ph_2)]$ in thf–MeO^2H. The thermal reactivity of the complex $[WH(SC_6H_2Me_3\text{-}2,4,6)_3(PMe_2Ph)_2]$ **3** was studied by combined TGA–mass spectrometry. The temperature for TGA started at 50 °C and was increased at 3° min^{-1} until 500 °C. Three events were seen at 200, 260 and 320 °C. At each, mesitylene, the hydrodesulfurisation product, was the major species detected by mass spectrometry; PMe_2Ph was also detected during the first event and $HSC_6H_2Me_3$-2,4,6 during the second and third events at low levels.

Hydrodesulfurisation of sulfurous contamination in feedstock is achieved by passing the feedstock and hydrogen gas over a metal catalyst at high temperatures and pressures. The most widely used catalyst is an alumina-supported molybdenum disulfide promoted by Co or Ni.[1–4] Hydrides have been implicated in the chemistry of the catalyst but as yet have not been detected unambiguously.[5,6] A number of mechanistic steps have been proposed in the degradation of typical substrates such as thiophene and butanethiol.[7–11] These substrates are considered to bind to a metal centre on the catalyst, then hydrogenolysis occurs *via* a common metal-bound butanethiolate intermediate which may leave the metal surface *via* S–C cleavage with or without further hydrogenolysis to form butane or butene, respectively. A possible step in the mechanism is transfer of hydrogen from the metal to a metal-bound thiolate, thus inducing S–C cleavage.[7,12]

The metal thiolate–hydride complexes which we have recently prepared[13–15] provide a means of assessing the propensity for cleavage of an S–C bond at a metal centre by hydrogen transfer. We have briefly reported that the complexes $[MoH(SC_6H_2Pr^i_3\text{-}2,4,6)_3(PR^1Ph_2)]$ **1** (R^1 = Me or Et) in tetrahydrofuran (thf)–MeOH decompose to give $C_6H_3Pr^i_3$-1,3,5 and the complexes $[\{Mo(SC_6H_2Pr^i_3\text{-}2,4,6)(OMe)(PR^1Ph_2)\}_2(\mu\text{-}S)_2]$ **2**.[13] This decomposition involves cleavage of an aryl S–C bond, which has relevance to hydrodesulfurisation, and here we describe this work and a study on related tungsten complexes in detail.

Results and Discussion

Molybdenum Systems.—During our studies of the complexes $[MoH(SC_6H_2Pr^i_3\text{-}2,4,6)_3(PR^1Ph_2)]$ **1** (R^1 = Me or Et)[13,14] and $[MH(SR)_3(PMe_2Ph)_2]$ **3** (R = $C_6H_2Pr^i_3$-2,4,6, or $C_6H_2Me_3$-2,4,6; M = Mo or W)[15,16] we found that complexes **1** (R = Me or Et) decompose at room temperature in the presence of methanol or ethanol, with carbon–sulfur bond cleavage,[13] to produce the complexes $[\{Mo(SC_6H_2Pr^i_3\text{-}2,4,6)(OR^2)(PR^1Ph_2)\}_2(\mu\text{-}S)_2]$ ($R^1 = R^2$ = Me **2a** or Et **2b**) as shown in Scheme 1. The absence of any metal–hydride stretching frequency in the infrared spectra of **2** indicated that decomposition had proceeded with loss of the hydride ligand. This was further confirmed by the proton-coupled ^{31}P NMR spectrum of **2a** in benzene which showed a singlet at δ −128.9. The ^1H NMR spectrum of **2a** shows two septets (2:1) in the chemical shift range δ 2–4 (*o*- and *p*-methyne resonances of the thiolate ligand) and phenyl resonances in the region δ 6–8 ($PMePh_2$); the spectrum of **2b** is similar.

The crystal structures of compounds **2a** and **2b** have been established by X-ray diffraction analyses.

Crystal Structures.—Crystals of complexes **2a** and **2b** are almost isostructural. Different views of their very similar structures are shown in Figs. 1 and 2. Selected bond dimensions are compared in Table 1.

The dimeric molecules of both structures are arranged about

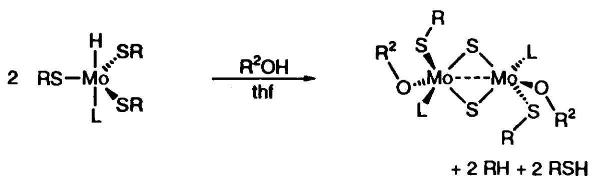

Scheme 1 Dimer formation. R = $C_6H_2Pr^i_3$-2,4,6, L = PR^1Ph_2, R^2 = Me or Et; thf = tetrahydrofuran

---

* *Supplementary data available:* See Instructions for Authors, *J. Chem. Soc., Dalton Trans.*, 1995, Issue 1, pp. xxv–xxx.

Non-SI unit employed: eV ≈ 1.60 × 10^{-19} J.

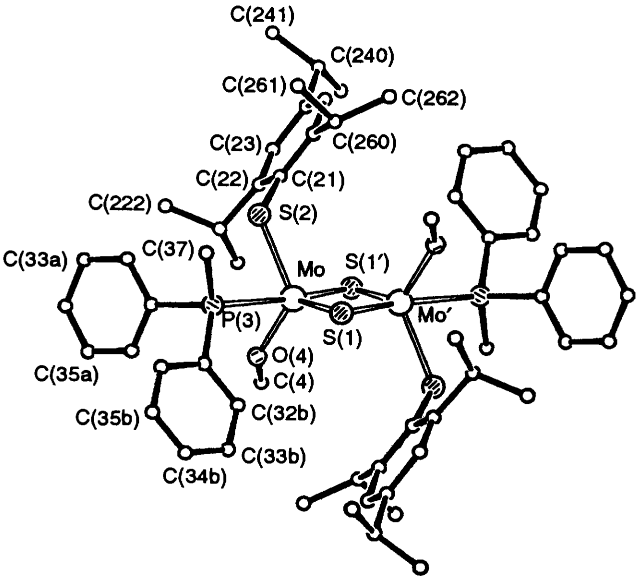

Fig. 1 Molecular structure of [{Mo(SC$_6$H$_2$Pr$^i_3$-2,4,6)(OMe)(PMePh$_2$)}$_2$(μ-S)$_2$] **2a**, indicating the atom numbering scheme; primed atoms are in the centrosymmetrically related half of the molecule

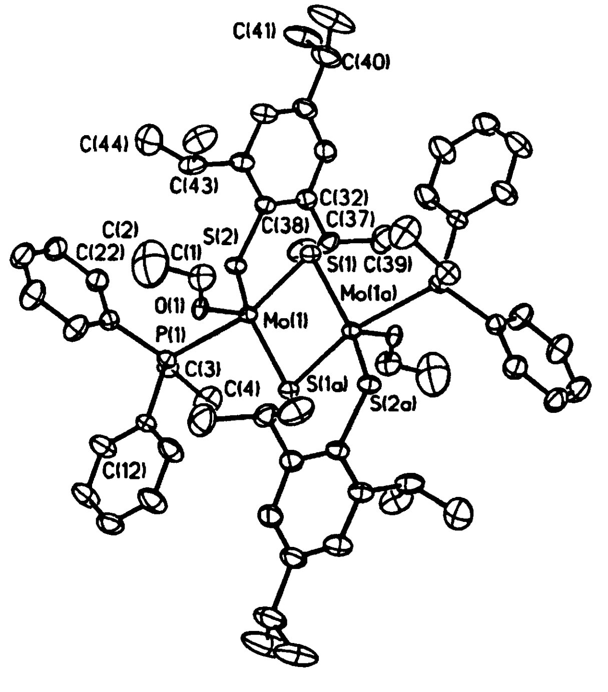

Fig. 2 Molecular structure of [{Mo(SC$_6$H$_2$Pr$^i_3$-2,4,6)(OEt)(PEtPh$_2$)}$_2$(μ-S)$_2$] **2b**, with the atom numbering scheme indicated. Atoms in the second half of the molecule are shown with the suffix 'a'

Table 1 Selected bond dimensions (distances in Å, angles in °) in [{Mo(SC$_6$H$_2$Pr$^i_3$-2,4,6)(OR)(PRPh$_2$)}$_2$(μ-S)$_2$] (R = Me **2a** or Et **2b**) with estimated standard deviations (e.s.d.s) in parentheses

2a		**2b**	
(*a*) In the Mo$_2$S$_2$ core			
Mo–Mo'	2.691(1)	Mo(1)–Mo(1a)	2.6970(10)
Mo–S(1)	2.231(2)	Mo(1)–S(1a)	2.228(3)
Mo–S(1')	2.354(2)	Mo(1)–S(1)	2.353(2)
Mo–S(2)	2.329(2)	Mo(1)–S(2)	2.347(2)
Mo–P(3)	2.578(2)	Mo(1)–P(1)	2.605(2)
Mo–O(4)	1.902(4)	Mo(1)–O(1)	1.902(6)
S(1)–Mo–S(1')	108.2(1)	S(1)–Mo(1)–S(1a)	107.9(1)
S(1)–Mo–S(2)	114.7(1)	S(1a)–Mo(1)–S(2)	116.2(1)
S(1')–Mo–S(2)	93.8(1)	S(1)–Mo(1)–S(2)	92.3(1)
S(1)–Mo–P(3)	85.1(1)	S(1a)–Mo(1)–P(1)	86.3(1)
S(1')–Mo–P(3)	166.7(1)	S(1)–Mo(1)–P(1)	165.8(1)
S(2)–Mo–P(3)	79.3(1)	S(2)–Mo(1)–P(1)	79.8(1)
S(1)–Mo–O(4)	117.0(1)	S(1a)–Mo(1)–O(1)	117.7(2)
S(1')–Mo–O(4)	94.6(1)	S(1)–Mo(1)–O(1)	94.0(2)
S(2)–Mo–O(4)	121.5(1)	S(2)–Mo(1)–O(1)	120.4(2)
P(3)–Mo–O(4)	79.7(1)	P(1)–Mo(1)–O(1)	80.0(1)
Mo–S(1)–Mo'	71.8(1)	Mo(1)–S(1)–Mo(1a)	72.1(1)
(*b*) In the benzenethiolate ligand			
S(2)–C(21)	1.785(7)	S(2)–C(31)	1.788(8)
Mo–S(2)–C(21)	117.9(2)	Mo(1)–S(2)–C(31)	117.1(2)
(*c*) In the phosphine ligand			
P(3)–C(31a)	1.831(7)	P(1)–C(11)	1.822(8)
P(3)–C(31b)	1.821(7)	P(1)–C(21)	1.812(11)
P(3)–C(37)	1.823(7)	P(1)–C(3)	1.840(10)
		C(3)–C(4)	1.51(2)
Mo–P(3)–C(31a)	109.7(2)	Mo(1)–P(1)–C(11)	120.1(2)
Mo–P(3)–C(31b)	119.1(3)	Mo(1)–P(1)–C(21)	108.9(3)
C(31a)–P(3)–C(31b)	101.6(3)	C(11)–P(1)–C(21)	102.6(4)
Mo–P(3)–C(37)	115.9(3)	Mo(1)–P(1)–C(3)	116.7(3)
C(31a)–P(3)–C(37)	106.0(4)	C(11)–P(1)–C(3)	102.7(4)
C(31b)–P(3)–C(37)	102.9(4)	C(21)–P(1)–C(3)	103.8(4)
		P(1)–C(3)–C(4)	111.6(6)
(*d*) In the alkoxide ligand			
O(4)–C(4)	1.407(8)	O(1)–C(1)	1.416(15)
		C(1)–C(2)	1.37(3)
Mo–O(4)–C(4)	132.8(5)	Mo(1)–O(1)–C(1)	132.4(5)
		O(1)–C(1)–C(2)	113.7(10)

crystallographic centres of symmetry. The co-ordination of the molybdenum atoms is basically trigonal bipyramidal, with P(3) and S(1') as the principal apices in complex **2a**, and P(1) and S(1) in **2b**. The equatorial planes comprise S(1), S(2) and O(4) in **2a**, and, correspondingly, S(1a), S(2) and O(1) in **2b**. The apical Mo–S distances are, as expected, rather longer than those in the equatorial plane. The thiolate ligands occupy their preferred equatorial site. The alkoxide ligands are both 'bent', with a mean Mo–O–C angle of 132.6(2)° the Mo–O distances are identical at 1.902 Å and typical of a single bond. The two Mo atoms are 2.691(1) and 2.697(1) Å apart in the two structures; these distances and the acute Mo–S–Mo angles (each *ca.* 72°) in the Mo$_2$S$_2$ cores indicate multiple metal–metal bonding, as would be expected for diamagnetic d^2–d^2 molybdenum(IV) systems.[17] The dimeric molecules are discrete moieties and separated from other molecules by normal van der Waals contacts.

These compounds are analogues of the complexes [{M(SBu^t)$_2$(PMe$_2$Ph)}$_2$(μ-S)$_2$] (M = Mo or W) formed by alkyl C–S cleavage of a thiolate ligand, as shown in reactions (1) and (2).[18,19] Comparable structural data for these complexes,

$$2\textit{cis}\text{-}[\mathrm{Mo(N_2)_2(PMe_2Ph)_4}] + 6\mathrm{Bu^tSH} \longrightarrow [\{\mathrm{Mo(SBu^t)_2(PMe_2Ph)}\}_2(\mu\text{-S})_2] + 4\mathrm{N_2} + 2\mathrm{H_2} + 2\mathrm{HBu^t} + 6\mathrm{PMe_2Ph} \quad (1)$$

$$2[\mathrm{Mo(SBu^t)_4}] + 2\mathrm{PMe_2Ph} \longrightarrow [\{\mathrm{Mo(SBu^t)_2(PMe_2Ph)}\}_2(\mu\text{-S})_2] + 2\mathrm{Me_2C{=}CH_2} + 2\mathrm{Bu^tSH} \quad (2)$$

for the analogue [{Mo(SBu^t)$_2$(NHMe$_2$)}$_2$(μ-S)$_2$],[20] and the structurally similar complex [{W(SePh)$_2$(PMePh$_2$)}$_2$(μ-Se)$_2$][21] are collected in Table 2. The M–M distances span the narrow

Table 2 Structural data (distances in Å, angles in °) for some $M_2(\mu\text{-}E)_2$ bridged dimeric complexes (M = Mo^{IV} or W^{IV}; E = S or Se)

Complex	M–M	M–S$_{ap}$[a]	M–S$_{eq}$[a]	M–S$_t$[a]	S–M–S′[b]	Ref.
[{Mo(SC$_6$H$_2$Pr$^i_3$-2,4,6)(OMe)(PMePh$_2$)}$_2$(μ-S)$_2$] **2a**	2.691(1)	2.354(2)	2.231(2)	2.329(2)	108.2(1)	This work
[{Mo(SC$_6$H$_2$Pr$^i_3$-2,4,6)(OEt)(PEtPh$_2$)}$_2$(μ-S)$_2$] **2b**	2.697(1)	2.353(2)	2.228(3)	2.347(2)	107.9(1)	This work
[{Mo(SBu^t)$_2$(PMe$_2$Ph)}$_2$(μ-S)$_2$]	2.741(1)	—	—	2.31[c]	—	19
[{W(SBu^t)$_2$(PMe$_2$Ph)}$_2$(μ-S)$_2$]	2.736(2)	2.345(7)	2.254(6)	2.313(5) 2.317(5)	107.0(2)	18
[{Mo(SBu^t)$_2$(NHMe$_2$)}$_2$(μ-S)$_2$]	2.730(1)	2.327(1)	2.238(1)	2.323(1)	106.5(1)	20
[{W(SePh)$_2$(PMePh$_2$)}$_2$(μ-Se)$_2$]	2.728(1)	2.473(1)[d]	2.380(2)[d]	2.438(2)[d] 2.461(2)[d]	111.6(1)[d]	21

[a] S$_{ap}$ = Apical sulfide, S$_{eq}$ = equatorial sulfide, S$_t$ = thiolate sulfur. [b] A centre of symmetry relates the two halves of the dimer in each structure. The M$_2$S$_2$ ring is therefore planar and the M–S–M′ angle is the complement of the S–M–S′ angle. [c] Mean value. [d] M–Se distances, Se–M–Se angle.

range 2.691–2.741 Å; clearly the distance is dominated by the metal–metal interaction and little affected by variation of the terminal or bridging ligands.

Mechanism of the S–C *Cleavage Reaction.*—The complex [{Mo(SC$_6$H$_2$Pr$^i_3$-2,4,6)(OMe)(PMePh$_2$)}$_2$(μ-S)$_2$] was formed as shown in equation (3). Methanol is essential for the S–C

$$2[\mathrm{MoH(SC_6H_2Pr^i{}_3\text{-}2,4,6)_3(PMePh_2)}] + 2\mathrm{MeOH} \xrightarrow{\text{thf}} [\{\mathrm{Mo(SC_6H_2Pr^i{}_3\text{-}2,4,6)(OMe)(PMePh_2)}\}_2(\mu\text{-S})_2] + 2\mathrm{HSC_6H_2Pr^i{}_3\text{-}2,4,6} + 2\mathrm{C_6H_3Pr^i{}_3\text{-}1,3,5} \quad (3)$$

cleavage reaction. This was shown by eliminating it from the reaction mixture, whereupon no cleavage occurred. The main organic products of this reaction are HSC$_6$H$_2$Pr$^i_3$-2,4,6 and triisopropylbenzene.

The course of the reaction was followed by deuterium labelling. The complexes [Mo^{2}H(SC$_6$H$_2$Pr$^i_3$-2,4,6)$_3$(PR^{1}Ph$_2$)][14] were dissolved in dry thf and their ^{2}H NMR spectra observed. The spectra, consisting of a doublet resonance due to the metal deuteride (δ 3.9, R^1 = Me; δ 3.1, R^1 = Et), were essentially unchanged for up to 2 weeks. Upon addition of MeO^{2}H to [MoH(SC$_6$H$_3$Pr$^i_3$-2,4,6)$_3$(PR′Ph$_2$)] the ^{2}H NMR spectra showed the immediate appearance of the signal at δ 3.7 due to MeO^{2}H and also of a resonance at δ 7.4 due to the formation of 2C$_6$H$_2$(^{2}H)Pr$^i_3$-1,3,5, *i.e.* the reactions proceed as shown in equation (4).

$$2[\mathrm{MoH(SC_6H_2Pr^i{}_3\text{-}2,4,6)_3(PMePh_2)}] + 2\mathrm{MeO^2H} \longrightarrow [\{\mathrm{Mo(SC_6H_2Pr^i{}_3\text{-}2,4,6)(OMe)(PMePh_2)}\}_2(\mu\text{-S})_2] + 2\mathrm{HSC_6H_2Pr^i{}_3\text{-}2,4,6} + 2\mathrm{C_6H_2(^2H)Pr^i{}_3\text{-}1,3,5} \quad (4)$$

The organic products of the decomposition reaction were also studied by GC–mass spectrometry. Test solutions of [MoH(SC$_6$H$_2$Pr$^i_3$-2,4,6)$_3$(PMePh$_2$)] in thf showed no traces of triisopropylbenzene until methanol was added. The other organic products detected were HSC$_6$H$_2$Pr$^i_3$-2,4,6, PMePh$_2$, and PSMePh$_2$ (see Experimental section). In the reaction of the metal hydride complex with deuteriated methanol the organic products detected by GC–mass spectrometry were C$_6$H$_2$(^{2}H)Pr$^i_3$-1,3,5 and HSC$_6$H$_2$Pr$^i_3$-2,4,6.

In a complementary experiment [Mo^{2}H(SC$_6$H$_2$Pr$^i_3$-2,4,6)$_3$(PEtPh$_2$)] with MeOH gave C$_6$H$_3$Pr$^i_3$-1,3,5 and HSC$_6$H$_2$Pr$^i_3$-2,4,6. The expected deuterium label in the latter product appeared to be diluted by exchange with the large excess of MeOH to a level that we could not detect.

Possible Mechanisms.—There are two possible mechanisms that account for the observations (Schemes 2 and 3). Both, we believe, involve prior co-ordination of methanol to form a six-co-ordinate adduct [MoH(SC$_6$H$_2$Pr$^i_3$-2,4,6)$_3$(R^{2}OH)(PMePh$_2$)]. We have already demonstrated the ease of formation of such adducts, *e.g.* [MoH(SC$_6$H$_2$Pr$^i_3$-2,4,6)$_3$(C$_5$H$_5$N)(PMePh$_2$)].[14] Metathesis of a methoxide for thiolate would then generate a more hydridic, sterically accessible hydride ligand. This would provide an explanation for the requirement of methanol. In Scheme 2 this activated hydride then attacks the S–C bond in an intramolecular step, forming triisopropylbenzene and a molybdenum sulfide complex, which subsequently dimerises. A related reaction is the addition of HSC$_6$H$_2$Pr$^i_3$ or HSC$_6$H$_2$Me$_3$ to W(OC$_6$H$_3$Me$_2$-2,6)$_4$ [equation (5)].[22] It is

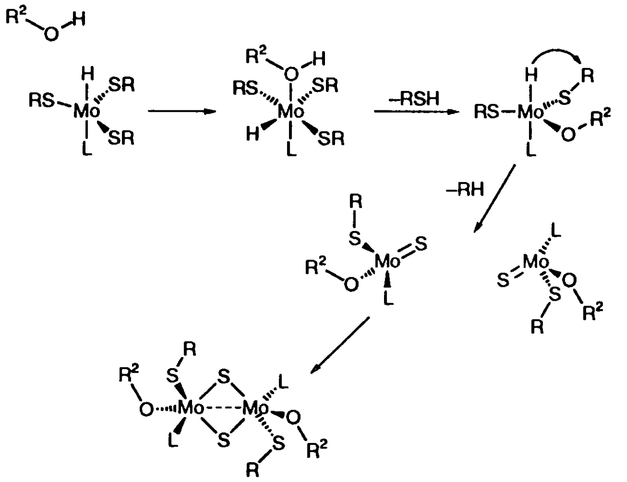

Scheme 2 Mechanism of S–C cleavage with intramolecular hydrogen-atom transfer; R = C$_6$H$_2$Pr$^i_3$-2,4,6

$$\mathrm{W(OC_6H_3Me_2\text{-}2,6)_4} + \mathrm{RSH} \longrightarrow [\mathrm{WS(OC_6H_3Me_2\text{-}2,6)_4}] + \mathrm{RH} \quad (5)$$

postulated that the mechanism of reaction (5) involves oxidative addition of the arenethiol to give a tungsten(VI) hydride intermediate; C–S bond cleavage is then proposed to occur *via* intramolecular hydride transfer, to give the products.[22]

The second possible mechanism for reaction (3) involves intermolecular attack by the activated hydride on the S–C bond of another molybdenum complex molecule (Scheme 3). Again, prior metathesis of methoxide for thiolate occurs, and the resulting more active species attacks the carbon–sulfur bond in a second equivalent of the metal complex. This mechanism is supported by the observation that hydride transfer from [Nb(C$_5$H$_5$)$_2$H$_3$] to molybdenum thiolate complexes leads to cleavage of alkyl–sulfur bonds, see reaction (6).[23] We have not

$$2[\mathrm{Nb(C_5H_5)_2H_3}] + [\mathrm{Mo(SBu^t)_4}] \longrightarrow [(\mathrm{C_5H_5})_2\mathrm{Nb}(\mu\text{-S})_2\mathrm{Mo}(\mu\text{-S})_2\mathrm{Nb}(\mathrm{C_5H_5})_2] + 4\mathrm{HBu^t} + \mathrm{H_2} \quad (6)$$

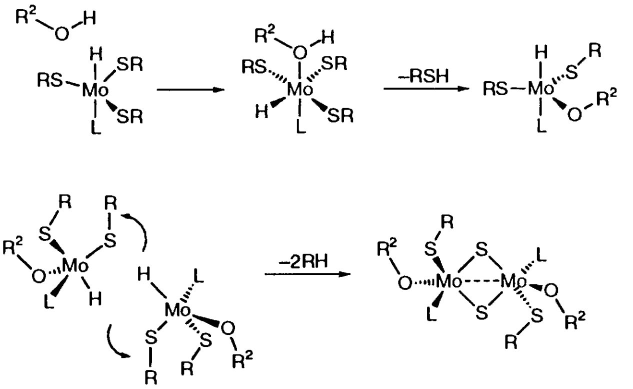

Scheme 3 Mechanism of S–C cleavage with intermolecular hydrogen-atom transfer; R = $C_6H_2Pr^i{}_3$-2,4,6

been able to determine whether the inter- or intra-molecular mechanism is operative in our case. Examples of aryl S–C scission are not common.

Tungsten Systems.—We have been unable to prepare tungsten analogues of the five-co-ordinate complexes **1** and have therefore studied the six-co-ordinate complexes [$WH(SC_6H_2Me_3$-2,4,6$)_3(PMe_2Ph)_2$] **3** and [$W^2H(SC_6H_2Me_3$-2,4,6$)_3(PMe_2Ph)_2$] **3D**.[15] Under thermal gravimetric analysis conditions these complexes also undergo C–S bond cleavage in the solid state. The thermal reactivity of **3** was studied by combined TGA–mass spectrometry. In repeated and reproducible reactions the temperature for TGA started at 50 °C and was increased at 3 ° min^{-1} until 500 °C. Three events were seen at 200, 260 and 320 °C (Table 3). At each of these events, mesitylene, the hydrodesulfurisation product, was the major species detected by mass spectrometry; PMe_2Ph was also detected during the first event and $HSC_6H_2Me_3$-2,4,6 during the second and third events at low levels. A black powder remained after these processes which contained C, H and S (microanalysis) but could not be formulated.

In a single preliminary experiment, the TGA of complex **3D** gave only two events at 180 and 230 °C under similar conditions. In the first $C_6H_2(^2H)Me_3$-1,3,5 was the major product, accompanied by lower yields of $C_6H_3Me_3$-1,3,5, PMe_2Ph, $HSC_6H_2Me_3$-2,4,6 and biphenyl. In the second event, smaller amounts of mesitylene, $C_6H_2(^2H)Me_3$-1,3,5 and $HSC_6H_2Me_3$-2,4,6 were lost. There are at least two explanations for the formation of these products. The first is intramolecular attack of hydride (deuteride) on the sulfur-bound carbon; this would explain why $C_6H_2(^2H)Me_3$-1,3,5 is the major product from **3D**. A second explanation would be the homolysis of a C–S bond followed by hydride (deuteride) abstraction by the mesityl radical thus formed; this could explain why $C_6H_3Me_3$-1,3,5 as well as $C_6H_2(^2H)Me_3$-1,3,5 is observed. Futher investigation was not undertaken at this stage.

There are other examples of C–S bond cleavage in thermolysis reactions, primarily involving bridging thiolates. The complex [$\{Cr(C_5H_5)(CO)(SPh)\}_2$] formed [$\{Cr(C_5H_5)(SPh)\}_2(\mu$-S)] after heating to 60 °C in thf for 2.5 h. The product, [$\{Cr(C_5H_5)(SPh)\}_2(\mu$-S)], heated at 110 °C in toluene for 24 h, gave [$Cr_4(C_5H_5)_4S_4$].[24] The hydride–thiolate cluster [$Ru_3(CO)_{10}(\mu$-SPh$)(\mu$-H)], when heated to 125 °C under 100 atm (*ca.* 10^7 Pa) of CO for 4 h in heptane, formed [$Ru_4(CO)_9(\mu$-CO$)_2(\mu_4$-S$)_2$] in 90% yield.[25] The homologous osmium cluster, [$Os_3(CO)_{10}(\mu$-SPh$)(\mu$-H)], formed [$Os_3(CO)_{12}$] (17%), [$Os_4(CO)_{13}(\mu_3$-S)] (27%), [$Os_5(CO)_{15}(\mu_4$-S)] (7%) and [$Os_3(CO)_9(\mu_3$-S$)_2$] (38%).[26,27] Two possibilities for C–S bond cleavage were considered for these complexes: either homolysis of the C–S bond occurs or an intramolecular metal-activated process. The intramolecular, metal-activated process is favoured for the C–S bond cleavage since, in the complex [$Os_3H(CO)_{10}(\mu$-SCH$_2$Ph)], C–S bond homolysis occurred to give hydride-containing osmium sulfide clusters and bibenzyl.[28] These products were not seen in the C–S bond cleavage of the benzenethiolate complexes.

Table 3 Thermal gravimetric–mass spectrometric data for [$WH(SC_6H_2Me_3$-2,4,6$)_3(PMe_2Ph)_2$]

T/°C	Mass loss (of original) (%)	Major organics (in order of abundance)
200	29.1	Mesitylene PMe_2Ph $HSC_6H_2Me_3$
260	10.3	Mesitylene $HSC_6H_2Me_3$
320	23.4	Mesitylene $HSC_6H_2Me_3$

The decomposition of $HSC_6H_2Me_3$-2,4,6 was also studied under similar conditions and showed a single event at 170 °C. The major mass spectral peaks were at *m/z* 302, 152 and 119 which correspond to the disulfide, the thiol and the fragment $C_6H_2Me_3$, respectively. Note that, for the decomposition studies, the peak for mesitylene occurred at *m/z* 120.

Conclusion

We have shown that the complexes [$MoH(SC_6H_2Pr^i{}_3$-2,4,6$)_3(PR^1Ph_2)$] in thf–R^2OH rapidly undergo C–S bond cleavage to give triisopropylbenzene and [$\{Mo(SC_6H_2Pr^i{}_3$-2,4,6$)(OR^2)(PR^1Ph_2)\}_2(\mu$-S$)_2$] and that the tungsten complex [$W^2H(SC_6H_2Me_3$-2,4,6$)_3(PMe_2Ph)_2$] undergoes C–S bond cleavage at 180 °C in the solid state to give $C_6H_2(^2H)Me_3$. The presence of a hydride on Mo or W appears to be important for the C–S bond-cleavage steps, which lends support for a hydride-transfer step in the mechanism of hydrodesulfurisation on industrial catalysts.

Experimental

All operations were performed under an atmosphere of dinitrogen. All solvents were dried and degassed before use. The molybdenum hydride starting materials were prepared by literature methods.[13,15,16] 2,4,6-Triisopropyl- and 2,4,6-trimethyl-benzenethiol were prepared by the method of Dilworth and co-workers.[29]

Spectroscopic measurements were made with JEOL GSX270 or Varian XL400 (NMR), Perkin-Elmer SP3-200 (IR) and Nicolet 5DX (FTIR) instruments. The ^{31}P and ^2H NMR spectra were referenced to $P(OMe)_3$ and natural-abundance deuterium in the solvent, respectively. Microanalyses were by Mr. C. J. Macdonald of the Nitrogen Fixation Laboratory or by Canadian Microanalytical Services.

Gas chromatographs were run on a Varian instrument using a DB-1 column (30 m long, 0.25 mm diameter; absorbent 0.25 µm thick). The injector temperature was 250 °C, the initial column temperature 100 °C and the detector temperature 300 °C. The temperature used was 100 °C for the first 10 min, then increased at 10° min^{-1} until 250 °C. Gas chromatography–mass spectrometry samples were run on an HP gas chromatograph interfaced to a VG 70-250S mass spectrometer using a 70 eV electron source.

Thermogravimetric results were obtained using a Perkin-Elmer 7 Series thermal analysis system interfaced to a Hewlett-Packard 5917A mass-selective detector by means of a thermostatted stainless-steel tube (1.2 m × 0.55 mm diameter). The input to the mass detector was a 0.3 m HP restrictor column in an HP 5890 GC oven. The column had a flow of 1 cm^3 min^{-1} with the remaining nitrogen flow split and vented. The mass detector used a 70 eV electron-impact ioniser, with a resolution of m/z 0.5 ± 0.05.

Preparation of $[\{Mo(SC_6H_2Pr^i_3\text{-}2,4,6)(OMe)(PMePh_2)\}_2(\mu\text{-}S)_2]$ **2a**.—The thiol $HSC_6H_2Pr^i_3$-2,4,6 (0.25 g, 1.08 mmol) was added to a stirred solution of $[MoH_4(PMePh_2)_4]$ (0.32 g, 0.34 mmol) in thf at 0 °C. The solution gradually changed from yellow to deep green over 2 h. The thf was removed in a vacuum at 20 °C and the resulting oily, slightly impure complex $[MoH(SC_6H_2Pr^i_3\text{-}2,4,6)_3(PMePh_2)]$ **1a** was pumped at 20 °C for 3 h to remove $PMePh_2$. The oil was then dissolved in MeOH (30 cm^3), filtered and allowed to stand at room temperature for 3 d to give dark green crystals of **2a** (0.17 g, 25%), which were suitable for structure determination. ^{31}P NMR (C_6H_6): δ −128.9 (Found: C, 62.3; H, 7.2. $C_{58}H_{78}Mo_2O_2P_2S_4$ requires C, 61.9; H, 7.0%).

The compound $[\{Mo(SC_6H_2Pr^i_3\text{-}2,4,6)(OEt)(PEtPh_2)\}_2(\mu\text{-}S)_2]$ **2b** was prepared in an identical fashion to **2a**, from $[MoH_4(PEtPh_2)_4]$, $HSC_6H_2Pr^i_3$-2,4,6 and EtOH. The product was dissolved in thf and the solution layered with ethanol to give brown crystals in 30% yield, which were suitable for structure determination.

Carbon–Sulfur Bond-cleavage Reactions.—$[MoH(SC_6H_2Pr^i_3\text{-}2,4,6)_3(PMePh_2)]$ *with* MeO^2H. (*a*) A solution of $[MoH(SC_6H_2Pr^i_3\text{-}2,4,6)_3(PMePh_2)]$ in dry thf (4 cm^3 of *ca.* 1 mmol dm^{-3} solution) was allowed to stand at room temperature for 24 h, after which its spectrum was unchanged. Deuteriomethanol MeO^2H (0.02 cm^3) was added and the ^2H NMR spectrum, observed within 5 min, showed the appearance of $^2HSC_6H_2Pr^i_3$-2,4,6 at δ 6.8. The organic products of the reaction were studied by GC–mass spectrometry; samples of the reaction solution, taken before addition of methanol, showed no trace of $C_6H_3Pr^i_3$-1,3,5. However, after addition of MeOH, $C_6H_3Pr^i_3$-1,3,5 was observed together with $PMePh_2$, $PSMePh_2$ and $HSC_6H_2Pr^i_3$-2,4,6. When MeO^2H was used as reagent, $C_6H_2(^2H)Pr^i_3$-1,3,5 was obtained (90% yield), together with $PMePh_2$, $PSMePh_2$ and $HSC_6H_2Pr^i_3$-2,4,6 in similar yield.

(*b*) *Control reaction.* A solution of $[Mo^2H(SC_6H_2Pr^i_3\text{-}2,4,6)_3(PMePh_2)]$ in dry thf (4 cm^3 of *ca.* 1 mmol dm^{-3} solution) was allowed to stand at room temperature for 2 weeks. The only ^2H resonance observed was that of Mo^2H at δ 3.9.

$[MoH(SC_6H_2Pr^i_3\text{-}2,4,6)_3(PEtPh_2)]$ *with* MeO^2H. In a 5 mm NMR tube, $[MoH(SC_6H_2Pr^i_3\text{-}2,4,6)_3(PEtPh_2)]$ (20 mg) was dissolved in dry thf (0.7 cm^3). One drop of MeO^2H (dried over 4 Å molecular sieves) was added. After 24 h the ^2H NMR spectrum showed peaks at δ 7.36, 3.30 and 1.75 corresponding to $C_6H_2(^2H)Pr^i_3$-1,3,5, MeO^2H and natural-abundance $[^2H]$thf, respectively. Gas chromatography–mass spectrometry showed that $C_6H_2(^2H)Pr^i_3$-1,3,5 was formed stoichiometrically.

A complementary experiment with $[Mo^2H(SC_6H_2Pr^i_3\text{-}2,4,6)_3(PEtPh_2)]$ and MeOH gave $C_6H_3Pr^i_3$-1,3,5 and $HSC_6H_2Pr^i_3$-2,4,6 (see text).

$[MoH(SC_6H_2Pr^i_3\text{-}2,4,6)_3(PEtPh_2)]$ *with* $^2H_2$. In a 5 mm NMR tube, $[MoH(SC_6H_2Pr^i_3\text{-}2,4,6)_3(PEtPh_2)]$ (45 mg) was dissolved in dry thf (0.7 cm^3). The sample was then put under a static $^2H_2$ atmosphere. The ^2H NMR spectrum was collected after 24 and 48 h. After 24 h a resonance was observed at δ 3.07 [$^2J(^2HP)$ 13.6 Hz] corresponding to Mo^2H. There were also peaks corresponding to naturally occurring $[^2H]$thf. After 48 h there was no change.

Solid-state Decomposition.—Thermogravimetric analysis of $[WH(SC_6H_2Me_3\text{-}2,4,6)_3(PMe_2Ph)_2]$. In a typical experiment, $[WH(SC_6H_2Me_3\text{-}2,4,6)_3(PMe_2Ph)_2]$ (14.533 mg) was placed in an aluminium pan in a TGA furnace and the system flushed with dinitrogen. The temperature of the furnace was raised to 50 °C and the temperature programme was started. In this case the temperature was increased at 3° min^{-1} until 450 °C. During the run the mass-selective detector was scanning from m/z 50 to 300. The transfer tubing and the GC oven were kept at 300 °C. The events, with mass loss and major peaks in the mass spectrum, are listed in Table 3.

Thermogravimetric analysis of $[W^2H(SC_6H_2Me_3\text{-}2,4,6)_3(PMe_2Ph)_2]$. (*a*) A sample of $[W^2H(SC_6H_2Me_3\text{-}2,4,6)_3(PMe_2Ph)_2]$ was run under similar conditions.

(*b*) *Control reaction.* A sample of $HSC_6H_2Me_3$-2,4,6 was run under the same conditions as those for the tungsten complexes.

Elemental Analysis of Residual Black Powders.—(*a*) *Produced at* 180 °C. A sample of $[WH(SC_6H_2Me_3\text{-}2,4,6)_3(PMe_2Ph)_2]$ (52 mg) was placed in a vial in a long slender Schlenk tube under dinitrogen. The end of the tube was placed in a silicon oil-bath, evacuated and heated to 180 °C for 4 h under dynamic vacuum. At the end of this period the sample was black. The mass remaining was 37 mg. The contents of the vial were found to contain, 42.85% C, 4.40% H and 13.85% S.

(*b*) *Produced at* 200 °C. A sample of $[WH(SC_6H_2Me_3\text{-}2,4,6)_3(PMe_2Ph)_2]$ (*ca.* 100 mg) was placed in a vial in a long slender Schlenk tube under dinitrogen. The end of the tube was placed in a silicon oil-bath and heated to 200 °C for 1 h under dinitrogen. At the end of this period the sample was black. The Schlenk tube was evacuated for 3 d, after which the contents of the vial were sent for analysis. There were two distinct types of material remaining: one was a black powder on the bottom of the vial and the other was a green-black oil on the side of the vial. The black powder contained 44.35% C, 4.70% H and 12.75% S and the green oil contained 42.10% C, 4.50% H and 9.50% S.

Crystal-structure Analyses.—The structure determinations of complexes **2a** and **2b** were carried out independently in different laboratories, **2a** in Sussex, **2b** in Toronto. Although the crystals are essentially isostructural, they are described by a different choice of cell parameters, different atom numbering schemes, *etc.*

$[\{Mo(SC_6H_2Pr^i_3\text{-}2,4,6)(OMe)(PMePh_2)\}_2(\mu\text{-}S)_2]$ **2a**. *Crystal data*: $C_{58}H_{78}Mo_2O_2P_2S_4$, $M = 1189.3$, triclinic, space group $I\bar{1}$ (equiv. to no. 2), $a = 10.921\,5(8)$, $b = 20.209(1)$, $c = 13.661(1)$ Å, $\alpha = 82.829(6)$, $\beta = 89.928(6)$, $\gamma = 97.148(6)°$, $U = 2967.8(4)$ Å^3, $Z = 2$, $D_c = 1.331$ g cm^{-3}, $F(000) = 1240$, μ(Mo-Kα) = 6.4 cm^{-1}, λ(Mo-Kα) = 0.710 69 Å.

The crystals are very dark, small rectangular plates and are air-sensitive. One was mounted on a glass fibre and coated with epoxy resin. After photographic examination, it was transferred to an Enraf-Nonius CAD4 diffractometer (with monochromated radiation) for determination of accurate cell parameters (from the settings of 24 reflections, θ *ca.* 10.5°, each reflection centred in four orientations) and measurement of diffraction intensities (to θ_{max} 20°).

During processing, intensities were corrected for Lorentz-polarisation effects, crystal deterioration (*ca.* 22% overall) and to ensure no negative intensities (by Bayesian statistical methods). 2756 Unique reflections were entered into the SHELX program system [30] for structure determination (by the heavy-atom method) and refinement (by full-matrix least-squares methods) to convergence with $R = 0.066$ and R_g [30] $= 0.047$ for all 2756 reflections weighted $w = \sigma_F^{-2}$. Hydrogen atoms were included in idealised positions; methyl groups were refined as rigid CH_3 groups and other hydrogen atoms were set to ride on their parent carbon atoms. The isotropic thermal parameters of all hydrogen atoms were refined independently. All the non-hydrogen atoms were allowed anisotropic thermal parameters. In a final difference map, the highest peaks were *ca.* 0.4 e Å^{-3} and close to the phosphorus atom.

Scattering factor curves for neutral atoms were taken from ref. 31. Computer programs used in the analysis have been noted above and in Table 4 of ref. 32, and were run on a DEC MicroVAX II machine. Final atomic coordinates are given in Table 4.

$[\{Mo(SC_6H_2Pr^i_3\text{-}2,4,6)(OEt)(PEtPh_2)\}_2(\mu\text{-}S)_2]$ **2b**. *Crystal*

Table 4 Final atomic coordinates (fractional × 10^4) for $[\{Mo(SC_6H_2Pr^i{}_3\text{-}2,4,6)(OMe)(PMePh_2)\}_2(\mu\text{-}S)_2]$ **2a** with e.s.d.s in parentheses

Atom	*x*	*y*	*z*
Mo	96.3(6)	− 662.1(3)	96.5(4)
S(1)	597(2)	36.3(9)	−1282(1)
S(2)	1771(2)	−963(1)	1027(1)
C(21)	1897(7)	−735(4)	2247(5)
C(22)	1152(7)	−1087(4)	3013(6)
C(220)	156(7)	−1668(5)	2856(6)
C(221)	−1087(8)	−1576(6)	3245(7)
C(222)	557(9)	−2330(5)	3309(9)
C(23)	1388(7)	−929(4)	3967(6)
C(24)	2313(8)	−436(5)	4167(6)
C(240)	2581(11)	−290(6)	5227(6)
C(241)	3181(15)	−829(7)	5812(8)
C(242)	1513(12)	−124(9)	5748(8)
C(25)	3017(7)	−105(4)	3398(6)
C(26)	2833(7)	−233(4)	2434(5)
C(260)	3697(7)	140(4)	1623(5)
C(261)	4819(9)	−216(5)	1495(8)
C(262)	4155(9)	865(4)	1745(8)
P(3)	791(2)	−1572(1)	−869(1)
C(31a)	416(7)	−2400(3)	−152(5)
C(32a)	1201(9)	−2652(5)	547(7)
C(33a)	835(11)	−3248(6)	1150(7)
C(34a)	−296(11)	−3583(5)	1035(7)
C(35a)	−1087(9)	−3347(5)	344(7)
C(36a)	−736(7)	−2749(5)	−238(6)
C(31b)	77(7)	−1706(4)	−2044(5)
C(32b)	−854(7)	−1359(4)	−2408(6)
C(33b)	−1422(8)	−1505(5)	−3273(6)
C(34b)	−1051(8)	−1989(5)	−3789(6)
C(35b)	−105(9)	−2323(5)	−3451(6)
C(36b)	450(8)	−2195(4)	−2569(6)
C(37)	2435(6)	−1490(6)	−1167(6)
O(4)	−1405(4)	−1251(2)	99(3)
C(4)	−2506(7)	−1320(6)	657(7)

Table 5 Final atomic coordinates (fractional × 10^4) for $[\{Mo(SC_6H_2Pr^i{}_3\text{-}2,4,6)(OEt)(PEtPh_2)\}_2(\mu\text{-}S)_2]$ **2b** with e.s.d.s in parentheses

Atom	*x*	*y*	*z*
Mo(1)	760(1)	3662(1)	546(1)
S(1)	−496(2)	5105(2)	−1331(2)
S(2)	2769(2)	2930(2)	−17(2)
P(1)	2346(2)	1621(2)	2475(2)
O(1)	−163(5)	2664(4)	951(4)
C(1)	−1240(9)	2783(10)	341(9)
C(2)	−1245(19)	1604(18)	721(16)
C(3)	4031(7)	1384(9)	2771(7)
C(4)	3993(9)	2491(11)	2902(11)
C(11)	1828(7)	1406(7)	3785(6)
C(12)	2662(9)	323(10)	4814(7)
C(13)	2274(10)	137(11)	5805(8)
C(14)	1009(10)	1017(10)	5792(8)
C(15)	196(10)	2054(11)	4799(8)
C(16)	578(9)	2269(10)	3793(8)
C(21)	2645(7)	105(7)	2515(6)
C(22)	3650(9)	−492(9)	2062(8)
C(23)	3827(10)	−1596(9)	2024(9)
C(24)	3002(11)	−2136(10)	2462(9)
C(25)	2017(10)	−1571(10)	2912(10)
C(26)	1860(8)	−473(9)	2954(9)
C(31)	2654(7)	3481(8)	−1485(6)
C(32)	3022(8)	4460(8)	−2138(7)
C(33)	3059(9)	4780(9)	−3249(7)
C(34)	2764(9)	4172(10)	−3720(7)
C(35)	2421(9)	3211(10)	−3068(8)
C(36)	2366(7)	2827(9)	−1937(7)
C(37)	3420(9)	5118(9)	−1650(8)
C(38)	4897(10)	4310(12)	−1102(11)
C(39)	3049(12)	6548(11)	−2466(11)
C(40)	2851(14)	4524(14)	−4943(9)
C(41)	4179(12)	3712(15)	−5018(10)
C(42)	1766(13)	4648(20)	−5612(11)
C(43)	2037(10)	1717(11)	−1260(8)
C(44)	3118(11)	418(12)	−1084(11)
C(45)	684(10)	2041(13)	−1820(11)

data. $C_{62}H_{86}Mo_2O_2P_2S_4$, $M = 1245.4$, triclinic, space group $P\bar{1}$ (no. 2), $a = 11.472(2)$, $b = 12.946(3)$, $c = 13.754(3)$ Å, $\alpha = 62.40(3)$, $\beta = 88.97(3)$, $\gamma = 63.98(3)°$, $U = 1582.1(8)$ Å^3, $Z = 1$, $D_c = 1.307$ g cm^{-3}, $F(000) = 652$, μ(Mo-Kα) = 6.0 cm^{-1}.

A transformation matrix (−1 0 0/1 −2 1/0 0 1) relates the primitive cell of complex **2b** to the *I*-centred cell (11.472, 20.156, 13.754 Å, 84.41, 91.03, 91.03°, $U = 3164.2$ Å^3), similar to the cell of **2a**.

For a small brown crystal, *ca.* 0.22 × 0.19 × 0.21 mm, accurate cell parameters were determined and intensity data measured by similar procedures to those described above, on a similar CAD4 diffractometer. Corrections for Lorentz-polarisation effects and absorption[33] were applied (there was no deterioration of the crystal) and 5055 unique reflections ($\theta_{max} = 25°$) were entered into the SHELXTL-PC program.[34] From an analysis similar to that above, the final R and wR[34] values were 0.069 and 0.087 for 4046 reflections (those with $I > 3\sigma_I$) weighted $w = (\sigma_F{}^2 + 0.0008F^2)^{-1}$. All the hydrogen atoms were included in idealised positions and set to ride on the parent carbon atoms with a common isotropic thermal parameter [U_{iso} refined to 0.131(7) Å^2]. The largest peaks in the final difference map were *ca.* 1.0 e Å^{-3} and close to the Mo atom.

All calculations were performed and the diagram generated with SHELXTL-PC running on a 486–66 computer. Final atomic coordinates are given in Table 5.

Additional material available from the Cambridge Crystallographic Data Centre comprises H-atom coordinates, thermal parameters and remaining bond lengths and angles

Acknowledgements

We thank the SERC for a studentship (to M. J. M), NATO for a collaborative research grant (to R. H. M and R. L. R), Natural Sciences and Engineering Research Council of Canada and Imperial Oil for operating grants (to R. H. M.), and Dr. M. Shiralian for preparing crystals of complex **2a**. We thank Mr. Charles Honeyman for operating the TGA and mass spectrometric instruments.

References

1 S. C. Schuman and H. Shalit, *Catal. Rev.*, 1970, **4**, 245.
2 F. E. Massoth, *Adv. Catal.*, 1978, **27**, 265.
3 M. B. Hocking, in *Modern Chemical Technology and Emission Control*, Springer, Berlin, 1985, p. 153.
4 C. J. Thompson, in *Organic Sulphur Chemistry*, 9th International Symposium Organic Sulphur Chemistry, IUPAC, Pergamon, Oxford, 1980, p. 189.
5 P. M. Boorman, K. J. Moynihan, V. D. Patel and J. F. Richardson, *Inorg. Chem.*, 1985, **24**, 2989.
6 R. J. Angelici, *Acc. Chem. Rev.*, 1988, **21**, 387.
7 B. C. Wiegand and C. M. Friend, *Chem. Rev.*, 1992, **92**, 491.
8 R. A. Sanchez-Delgado, *J. Mol. Cat.*, 1994, **86**, 287.
9 W. D. Jones and R. M. Chin, *J. Organomet. Chem.*, 1994, **472**, 311.
10 M. D. Curtis, *Appl. Organomet. Chem.*, 1992, **6**, 429.
11 J. B. Chen, L. M. Daniels and R. J. Angelici, *J. Am. Chem. Soc.*, 1991, **113**, 2544.
12 J. T. Roberts and C. M. Friend, *J. Am. Chem. Soc.*, 1986, **108**, 7204; 1987, **109**, 4423.
13 T. E. Burrow, A. Hills, D. L. Hughes, J. D. Lane, N. J. Lazarowych, M. J. Maguire, R. H. Morris and R. L. Richards, *J. Chem. Soc., Chem. Commun.*, 1990, 1757.
14 D. L. Hughes, N. J. Lazarowych, M. J. Maguire, R. H. Morris and R. L. Richards, *J. Chem. Soc., Dalton Trans.*, 1995, 5.

15 T. E. Burrow, A. Hills, D. L. Hughes, J. D. Lane, R. H. Morris and R. L. Richards, *J. Chem. Soc., Dalton Trans*, 1991, 1813.

16 T. E. Burrow, A. Hills, D. L. Hughes, J. D. Lane, A. J. Lough, R. H. Morris and R. L. Richards, *J. Chem. Soc., Dalton Trans.*, 1991, 2519.

17 F. A. Cotton and R. A. Walton, *Multiple Bonds Between Metal Atoms*, Wiley, New York, 1982.

18 P. Dahlstrom, J. R. Dilworth, J. Hutchinson, S. Kumar, R. L. Richards and J. A. Zubieta, *J. Chem. Soc., Dalton Trans.*, 1983, 1489.

19 T. Higuchi, K. Hirotsu, K. Kamata, S. Otsuka and T. Yoshida, *J. Am. Chem. Soc.*, 1981, **103**, 3572.

20 M. H. Chisholm, J. F. Corning and J. C. Huffman, *Inorg. Chem.*, 1982, **21**, 296.

21 P. M. Boorman, H.-B. Kraatz and M. Parvez, *J. Chem. Soc., Dalton Trans.*, 1992, 3281.

22 M. L. Listermann, R. R. Schrock, J. T. Dewan and R. M. Kolodziej, *Inorg. Chem.*, 1988, **27**, 264.

23 P. M. Boorman, J. F. Fait and G. Freeman, *Polyhedron*, 1989, **8**, 1762.

24 L. Y. Goh and M. S. Tay, *Organometallics*, 1992, **11**, 1711.

25 R. D. Adams, J. E. Babin and M. Tasi, *Inorg. Chem.*, 1986, **25**, 4514.

26 R. D. Adams and L.-W. Yang, *J. Am. Chem. Soc.*, 1982, **104**, 4115.

27 R. D. Adams, I. T. Horvath, B. E. Segmuller and L.-W. Yang, *Organometallics*, 1983, **2**, 1301.

28 R. D. Adams, I. T. Horvath, P. Mathur and B. E. Segmuller, *Organometallics*, 1983, **2**, 996.

29 P. J. Blower, J. R. Dilworth, J. P. Hutchinson and J. A. Zubieta, *J. Chem. Soc., Dalton Trans.*, 1985, 1533.

30 G. M. Sheldrick, SHELX 76, Program for crystal structure determination, University of Cambridge, 1976; also SHELXN, an extended version of SHELX 76, 1977.

31 *International Tables for X-Ray Crystallography*, Kynoch Press, Birmingham, 1974, vol. 4, pp. 99 and 149.

32 S. N. Anderson, R. L. Richards and D. L. Hughes, *J. Chem. Soc., Dalton Trans.*, 1986, 245.

33 N. Walker and D. Stuart, *Acta Crystallogr., Sect. A* 1983, **39**, 158.

34 G. M. Sheldrick, SHELXTL-PC, Siemens Analytical X-Ray Instruments, Madison, WI, 1990.

Received 6th *February* 1995; *Paper* 5/00669D